



# A critical study on the magnetic properties of ultrafine cobalt ferrite nanoparticles synthesized by polyethylene glycol assisted sol–gel method

G. R. Patta<sup>1,2</sup> · V. Ravi Kumar<sup>1</sup> · B. V. Ragavaiah<sup>3</sup> · N. Veeraiah<sup>1</sup>

Received: 12 November 2019 / Accepted: 19 December 2019 / Published online: 2 January 2020  
© Springer-Verlag GmbH Germany, part of Springer Nature 2020

## Abstract

High coercive single-domain  $\text{CoFe}_2\text{O}_4$  nanoparticles with the minimal average size (7.6–12.8 nm) were synthesized by polyethylene glycol (PEG) assisted sol–gel method and subsequent annealing at different temperatures. The prepared samples were characterized by XRD, TEM, TG-DSC, and FTIR techniques. The XRD and TEM studies indicated the size and shape of the particles are highly dependent on annealing temperature. Magnetic properties of the developed cobalt ferrite nanoparticles were found to be dependent on their size and shape. The particles annealed at lower temperatures (about 400 °C) are found to be near spherical in shape and as the annealing temperature is increased from 400 to 800 °C, the shape of the particles is observed to be transformed from spherical to octahedron through intermediate cubic shape. Magnetic parameters viz., saturation magnetization ( $M_s$ ) and remnant magnetization ( $M_r$ ) exhibited a study increase with increase of the particle size. The coercive field,  $H_c$  exhibited a non-monotonic behavior with distinct maximum at about 700 °C and suggested the transition from single-domain to multi-domain state. The magneto-crystalline anisotropy constant,  $K$ , determined from Stoner–Wohlfarth relation, exhibited the maximum value,  $10.74 \times 10^6 \text{ erg/cm}^3$  for the samples annealed at 800 °C. In addition, the magnitude of  $(\text{BH})_{\text{max}}$  (which is considered as the efficiency of cobalt ferrite nanoparticles for using as permanent magnets) exhibited the maximum value ( $1.04 \times 10^6 \text{ GOe}$ ). Such higher values of these two parameters suggest the possible applications of the studied material in magnetic recording, high density digital recording disks and in magnetic sensors.

**Keywords** Cobalt ferrite nanoparticles · Polyethylene glycol · High coercivity and high magnetization · Transition of geometrical shape

## 1 Introduction

Research in the field of nanoscale magnetic materials attracted much attention in the recent years due to their superior magnetic properties over those of corresponding bulk counterparts [1, 2]. For this reason, nanoscale magnetic materials find versatile applications, e.g., in electronics [3], in automobiles [4], in sensors [5], as actuators [6], as

electromagnetic wave absorbers [7, 8], as recyclable photo catalysts [9], in magnetic recording disks [10] and in several biomedical applications [11]. The research in the field of magnetic nanoparticles (MNP) has further been accelerated with the development of single-domain state of the magnetic particles by Frenkel and Dorfman [12].

It is well established fact that the magnetic properties of the nanomagnetic material are sensitive to shape and particle size as well as their site occupancy (viz., tetrahedral and octahedral sites) [13]. Recently, there has been a quest for new methods to develop magnetic ferrites to the nanoscale dimensions with superior magnetic properties. For example, they are anticipated to exhibit higher magnetization,  $M_s$ , if the material transforms from multi-domain to single-domain state [14]. Further, if the dimensions of the material are in the nanoscale, the surface anisotropy (size dependent), shape anisotropy (morphology controlled) and magnetostriction (strain induced) contribute additionally to its

✉ V. Ravi Kumar  
vrksurya@rediffmail.com

<sup>1</sup> Department of Physics, Acharya Nagarjuna University, Nagarjuna Nagar, Guntur 522510, India

<sup>2</sup> Department of Physics, Rajiv Gandhi University of Knowledge Technologies, IIIT, Nuzvid 521202, India

<sup>3</sup> Department of Physics, Rajiv Gandhi University of Knowledge Technologies, IIIT, Ongole 523001, India

intrinsic anisotropy; as a result, a considerable improvement of the magnetic performances of the material is expected. However, in the nanosized magnets (even though their magnetic anisotropy is high) there will be a significant reduction in the magnitude of magnetization ( $M_s$ ) due to thermal demagnetization. Therefore, the method of development of novel nanoscale magnetic materials with relatively higher magnetization needs a careful tailoring of the particle size by minimizing the thermal demagnetization effects and to confine particles into single-domain state [15].

Among various nanomagnetic materials, cobalt ferrite is well known due to its high coercivity, moderate magnetization and large cubic magneto-crystalline anisotropy along with its high physical and chemical stability [15–17]. In recent years, several methods of synthesis were adopted by several researchers to prepare highly crystalline and uniform sized cobalt ferrite nanoparticles [18–24]. However, most of these methods are not cost effective and not applicable for the production of nanosized magnets to a large scale. These methods require expensive and often toxic reagents and the synthetic steps are highly complicated. Further these methods need high reaction temperature [25] which is a hindrance for obtaining particles of nanosize [26]. Among different methods, sol–gel method is proven to be superior for the large-scale production of nanocrystalline materials at the easily adoptable optimum conditions [26, 27]. However, these nanoparticles show relatively low magnetization (Table 1) when compared to that of bulk cobalt ferrite sample (86 emu/g) [28] and also suffer with lower degree of crystallinity. Hence, there is a need to explore low temperature synthesis technique for the development of higher degree of crystallinity [29] (preferably below the single-domain state) with higher magnetization for not only biomedical applications and also for the various other technological applications.

Quite recently, we have developed the cobalt ferrite nanoparticles through PVP (polyvinylpyrrolidone) assisted

sol–gel method [26]. The grown particles (with the size more than 20 nm obtained at the annealing temperature 1000 °C) have exhibited 79.8 emu/g maximal saturation magnetization. The obtained particles are also found to be agglomerated and the cobalt ferrite phase is found to be initiated at relatively lower reaction temperature (~400 °C). With an objective, to obtain cobalt ferrite nanoparticles of uniform shape (in single-domain) at still lower dimensions (<20 nm) with higher degree of dispersion at relatively lower reaction temperature and with improved saturation magnetization, in this study, we have synthesized cobalt ferrite nanoparticles with an alternative chelating agent viz., polyethylene glycol (PEG) and reported their structural and magnetic properties.

## 2 Experimental

Stoichiometric amounts of AR grade ferric nitrate,  $\text{Fe}(\text{NO}_3)_3 \cdot 9\text{H}_2\text{O}$  and cobalt nitrate,  $\text{Co}(\text{NO}_3)_2 \cdot 6\text{H}_2\text{O}$  were taken to synthesize cobalt ferrite. Polyethylene glycol (PEG) was used as capping/chelating agent to monitor the size and shape of growing particles. Motivated by the previous studies, the ratio of amount of PEG and cobalt ferrite was maintained at 3:1 [26]. Solutions of metallic nitrates and PEG were prepared by dissolving them separately in a minimum quantity of de-ionized water with continuous stirring until a colorless, transparent solution was achieved at ambient temperature. Resulting mixture of the solution was heated at 80 °C in air with vigorous stirring for 15 h. The obtained gel was further heated at 80 °C in air for nearly 10 h. Subsequently, the densified gel was annealed at various temperatures in the range 300–800 °C.

The structural analysis of the samples was carried out using several experimental characterization techniques. However, one needs quantitative analysis of the structure of the material using first-principles electronic structure calculations with the Perdew–Burke–Ernzerhof (PBE) parameterization of the generalized gradient approximation (GGA) to density functional theory (DFT) as has been carried out by Ellen et al., for some alloys [30]. Such calculations for the studied material in the present case could not be performed. Our analysis is simply based on qualitative experimental techniques mentioned below.

BRUKER (D8 ADVANCE) X-ray diffractometer (XRD) (Cu K $\alpha$  radiation) along with a software called EVA is used to estimate the phase purity and the crystallite size of the annealed samples. TG-DSC analysis was performed using a NETZSCH STA 449 F3 Jupiter scanning calorimeter from room temperature to 1400 °C with heating rate 20 °C/min. A vertex 80 FTIR spectrophotometer was used to record infrared (IR) spectra of the samples in the wavenumber region 400–3000  $\text{cm}^{-1}$  to a precision of 0.2  $\text{cm}^{-1}$ . A Tecnai G2 20 S-Twin transmission electron microscope was used for

**Table 1** The reported values of particle size and magnetization of single-domain  $\text{CoFe}_2\text{O}_4$  nanoparticles

Annealing temp. (°C)	Particle size (nm)	$M_s$ (emu/g)	References
350	12	40	[50]
450	26	49	[51]
800	14	48	[52]
500	30	70.9	[53]
550	29	10	[34]
250	26	63	[54]
600	20	74	[55]
700	6.5	60	[40]
800	13	77.5	[26]

recording transmission electron microscopy (TEM) pictures of the samples. Vibrating sample magnetometer (Lakeshore Model 4700 VSM) was used for studying the magnetic properties of  $\text{CoFe}_2\text{O}_4$  nanoparticles at room temperature under a maximum applied field of 18 kOe.

### 3 Results and discussion

#### 3.1 X-ray diffraction (XRD) analysis

To identify the lowest optimal annealing temperature at which the pure phase of cobalt ferrite nanoparticles with least possible size could be achieved, the prepared samples were annealed at different temperatures in the range 300–800 °C (in the intervals of 100 °C) and their XRD patterns were recorded at each annealing temperature. The diffractogram of the sample annealed at 300 °C is presented in Fig. 1. Even though, the diffractogram exhibited the peaks corresponding to spinel structured cobalt ferrite phase, it also exhibited several auxiliary peaks corresponding to secondary oxide phases. As the annealing temperature is increased gradually upto 400 °C, the secondary peaks virtually vanished and the dominant peaks corresponding to single phase of cobalt ferrite (cubic spinel) [26] could clearly be visualized (pattern ‘a’ in Fig. 2). The diffractograms of the samples annealed at other temperatures (400 °C, 600 °C, 700 °C, and 800 °C) are presented in Fig. 2. The comparison of the diffractograms indicated increased intensity of the peaks corresponding to single phase cobalt ferrite with reduced half width with increase of annealing temperature. This behavior of the diffractograms indicates the increasing size of the crystallites as well as coagulation of particles

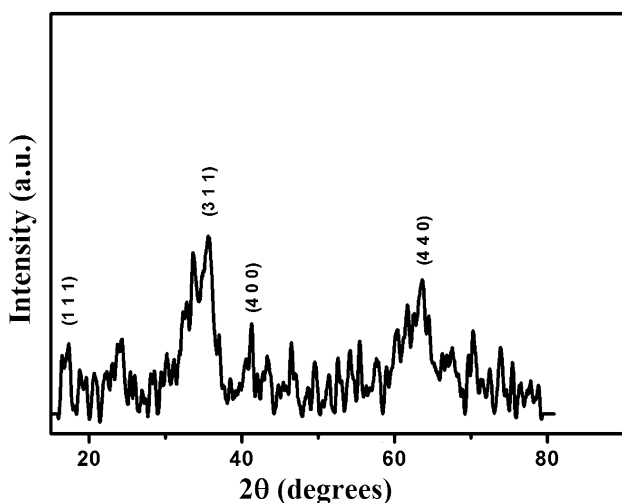


**Fig. 1** X-Ray diffractogram of cobalt ferrite sample annealed at 300 °C

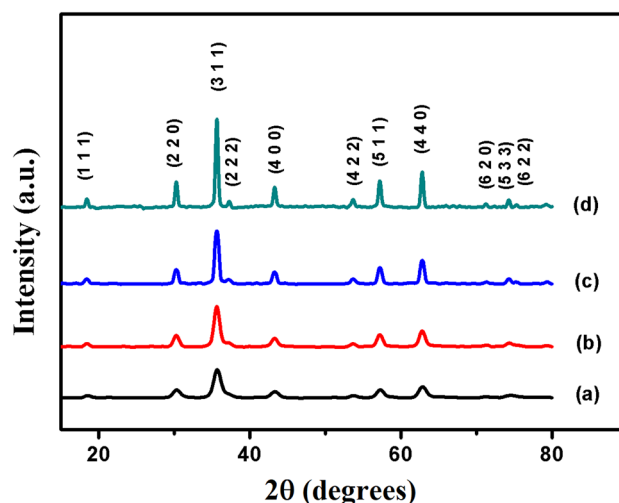


**Fig. 2** X-Ray diffraction patterns of cobalt ferrite sample annealed at **a** 400 °C, **b** 600 °C, **c** 700 °C, **d** 800 °C

[31]. We have estimated crystallite size by drawing  $\beta \cos \theta$  vs  $4\epsilon \sin \theta$  as per Williamson–Hall’s equation (W–H)

$$\beta \cos \theta = \frac{0.9\lambda}{D} + 4\epsilon \sin \theta. \quad (1)$$

In the Eq. (1),  $D$  represents the crystallite size, whereas  $\beta$  represents the corrected peak broadening estimated  $\sqrt{\beta_{\text{measured}}^2 - \beta_{\text{instrumental}}^2}$ ; details of other parameters can be found in Ref. [32]. Average crystallite sizes calculated using W–H diagrams (Fig. 3) are observed to be varying from 8.6 to 12.8 nm with increase of annealing temperatures 400 to 800 °C (Table 2). The lattice constant for all the samples was estimated by minimizing systematic and random errors using the Nelson–Riley extrapolation method [33]. The accurate value of lattice constant of each sample was obtained by extrapolating the plot between the calculated lattice constant and the Nelson–Riley function  $F(\theta) = (\cos^2 \theta / 2 \sin \theta) + (\cos^2 \theta / 2 \theta)$  (Fig. 4) of each plane from the diffraction pattern to the Y-axis. The value of lattice constant of the cubic structured  $\text{CoFe}_2\text{O}_4$  samples calculated from these diagrams is found to be  $\sim 8.39$  Å; this value is found to be nearly independent on annealing temperature and observed to be in good agreement with that of reported value prepared by different methods [31].

#### 3.2 FTIR analysis

FTIR spectral studies of the samples have been carried out to ascertain formation of  $\text{CoFe}_2\text{O}_4$  phase (with possible presence of Fe ions in octahedral sites). Figure 5 represents the FTIR spectra of the samples annealed at three specific

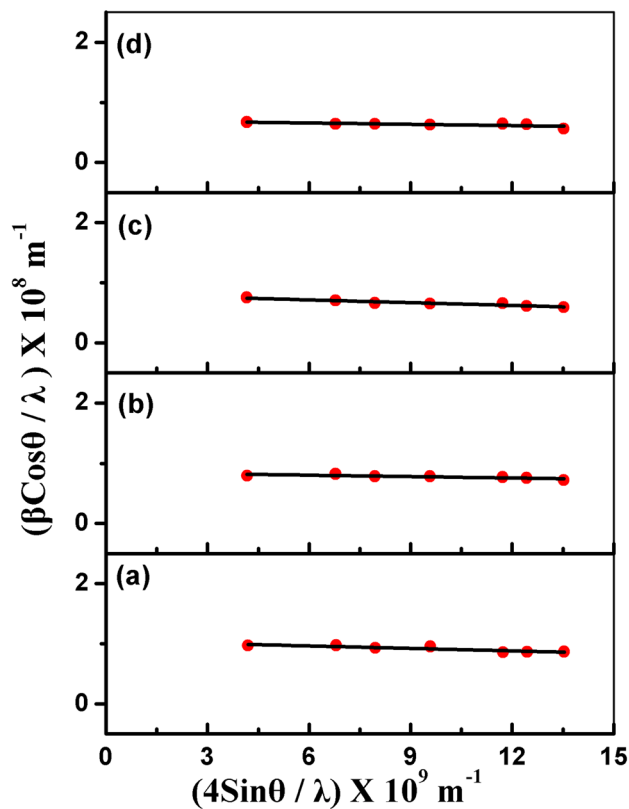


**Fig. 3** Williamson–Hall plots of cobalt ferrite samples annealed at **a** 400 °C, **b** 600 °C, **c** 700 °C, **d** 800 °C

temperatures viz., 300 °C, 400 °C, and 600 °C. Octahedral vibrational band of Fe–O bond is detected at about 587  $\text{cm}^{-1}$  [31, 34, 35] in the spectra of all the samples, whereas the tetrahedral vibrational band of Co–O bond is detected at about 420  $\text{cm}^{-1}$  [36]. Multiple feeble vibrational bands assigned to stretching-modes of C=H, O–H, and C–O groups of PEG [37] are also visualized (in the region of 1200–3000  $\text{cm}^{-1}$ ) in the spectra of the samples annealed at lower temperatures. Vibrational bands of O–H groups and also of C–O groups seemed to be gradually vanished with increasing the annealing temperature. The band representing exclusive vibrations  $\text{FeO}_6$  structural groups with increased intensity could clearly be visualized as the annealing temperature of the samples is increased.

### 3.3 TEM analysis

In Fig. 6, typical bright field TEM images, the selected area diffraction (SAD) patterns and the corresponding particle size histograms (of the particle population of not less than 100 in each case) of the cobalt ferrite nanoparticles annealed at different temperatures (in the region 400–800 °C) are presented. The histograms obtained from TEM images for evaluating the average particle diameter could be well fitted by a Gaussian distribution. The images of the sample annealed at 400 °C indicated that ultrafine nanoparticles present in the sample are in spherical shape with average diameter of  $7.6 \pm 0.9$  nm. Further, comparison of the TEM images of the samples annealed at different temperatures indicated that the size and shape of the particles is strongly dependent on the annealing temperature. To be more precise, in the samples annealed at lower temperatures, the particles are near spherical in shape and as the temperature of annealing is increased from 400 to 800 °C, transformation of the shape from spherical to octahedron through intermediate cubic shape could clearly be visualized. Such type of transformations of shape of these particles was also reported earlier by Alberto et al. [13]. The average particle sizes (edge to edge length) evaluated from these histograms (Fig. 6) of the particle size distribution were found to be in the range of 7.6–12.8 nm for the samples annealed from 400 to 800 °C (Table 2). The crystallite size, calculated from the X-ray diffraction patterns using W–H plots, are in good agreement with those obtained from TEM images; this inference further reinforces the argument that the developed particles in the annealed samples are of nanosized mono-crystallites. To ascertain the presence of all the elements in the particles we have recorded energy dispersive spectra (EDS) for these samples. In Fig. 7 EDS spectrum for one of the samples (sample annealed at 400 °C) is presented. The spectrum clearly suggested all the elements are quite intact in the sample even after annealing at higher temperature.

### 3.4 TG-DSC analysis

Figure 8 presents the thermogram of as prepared dark brown gel (composition of the ingredients) recorded in the temperature range 30–1300 °C. The thermogram exhibited alternate

**Table 2** Structural and magnetic parameters of cobalt ferrite nanoparticles annealed at different temperatures

Annealing temperature (°C)	Particle size (nm)	Crystallite size (nm)	$M_s$ (emu/g)	$M_r$ (emu/g)	$H_c$ (Oe)	$R = M_r/M_s$	$K$ ( $\times 10^6$ erg/cm <sup>3</sup> )
400	$7.6 \pm 0.9$	8.6	31.8	11.6	1543	0.36	3.21
600	$9.2 \pm 0.8$	10.5	60.4	26.2	1901	0.43	7.51
700	$10.2 \pm 0.4$	11.1	65.3	32.6	2214	0.50	9.46
800	$12.8 \pm 0.4$	12.8	85.5	49	1920	0.57	10.74

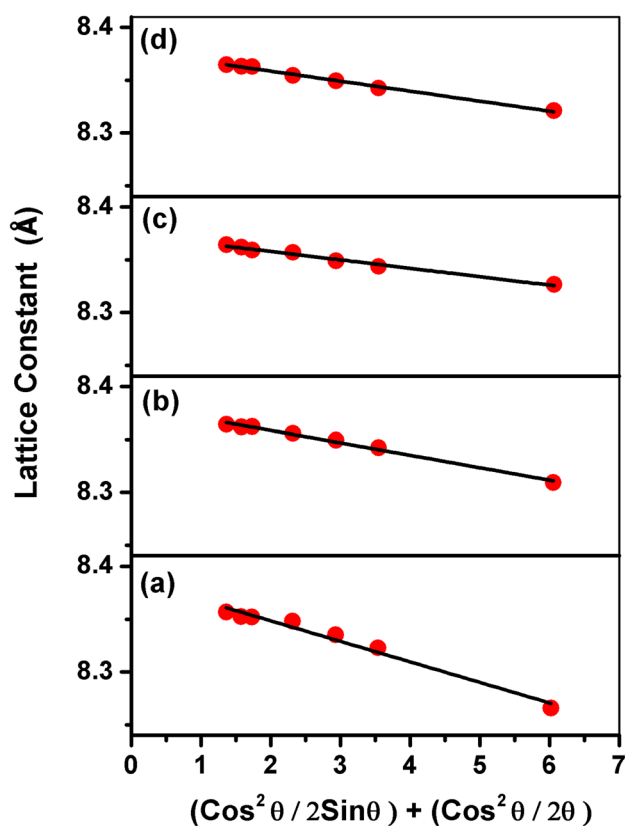


**Fig. 4** Nelson–Riley plots of cobalt ferrite samples annealed at **a** 400 °C, **b** 600 °C, **c** 700 °C, **d** 800 °C

endothermic and exothermic changes; the endothermic effects are observed at 215.4 °C, 412.6 °C, and 567.5 °C while the exothermic changes are noticed at 380.6 °C and 490.8 °C. The thermal gravimetry analysis indicated negligible weight loss up to about 200 °C and further increase of temperature, a gradual weight loss is observed in multiple steps in accordance with DSC traces. The weight loss is found to be nearly 70% at about 600 °C and beyond this temperature of annealing the samples were found to be nearly free from hydroxyl and carbonate groups. To be more specific, the first endothermic change observed at about 215 °C (at where the weight loss ~ 10%) can be ascribed to decomposition of nitrates [38] in the samples, whereas the subsequent exothermic effect observed at about 380 °C (accompanied by a near weight loss of 45%) is predicted to be connected with thermal degradation of PEG chains into CO<sub>2</sub> and H<sub>2</sub>O. The successive endothermic effects observed in the thermograms at 412 °C and 567 °C represent crystallization of cobalt ferrite nanoparticles [39] and magnetic ordering of nanoparticles, respectively. The second exothermic peak observed at about 490 °C (at where the weight loss is about 60%), is possibly due to combustion of the residual macromolecule (cineration process) [39]. A feeble endothermic peak is also visualized in the DSC trace at about

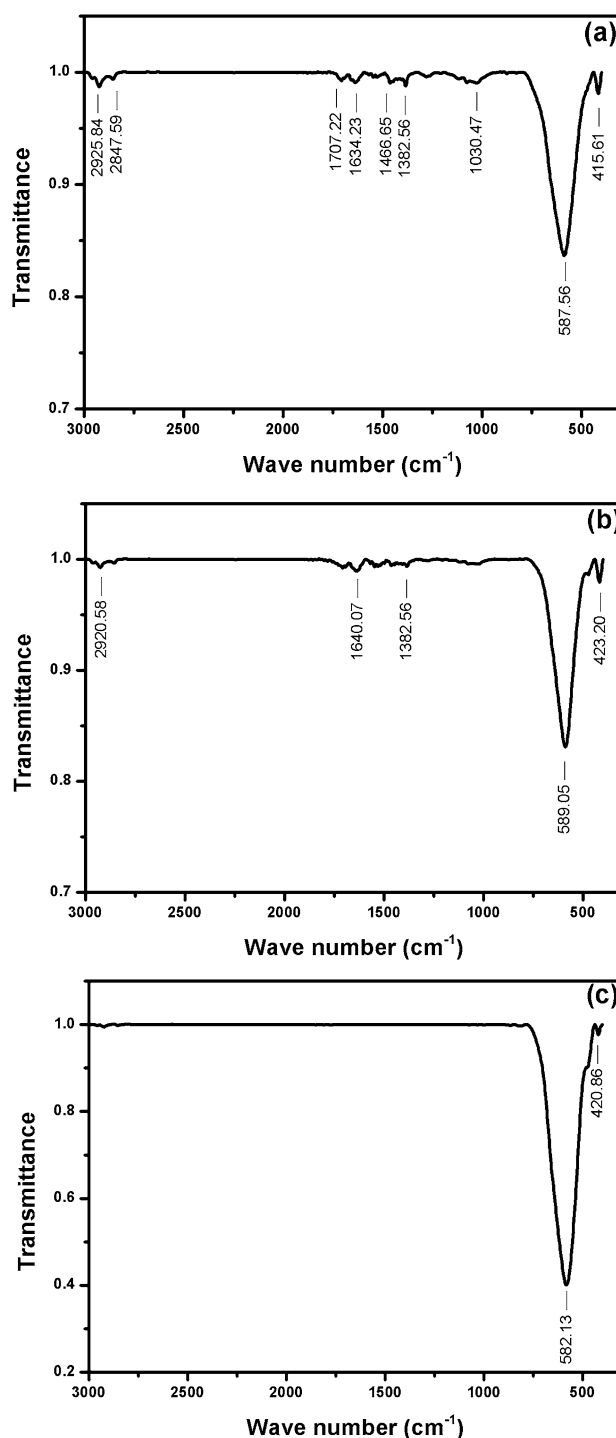


**Fig. 5** FTIR spectra of cobalt ferrite samples annealed at **a** 300 °C, **b** 400 °C, **c** 600 °C

1100 °C; this peak is predicted to be connected with microstructure changes (shrinkage of the sample) that would lead to enhancement of the density of the sample [40]. It may also be worth mentioning here that the changes observed in the thermograms of the sample are well in supportive of the

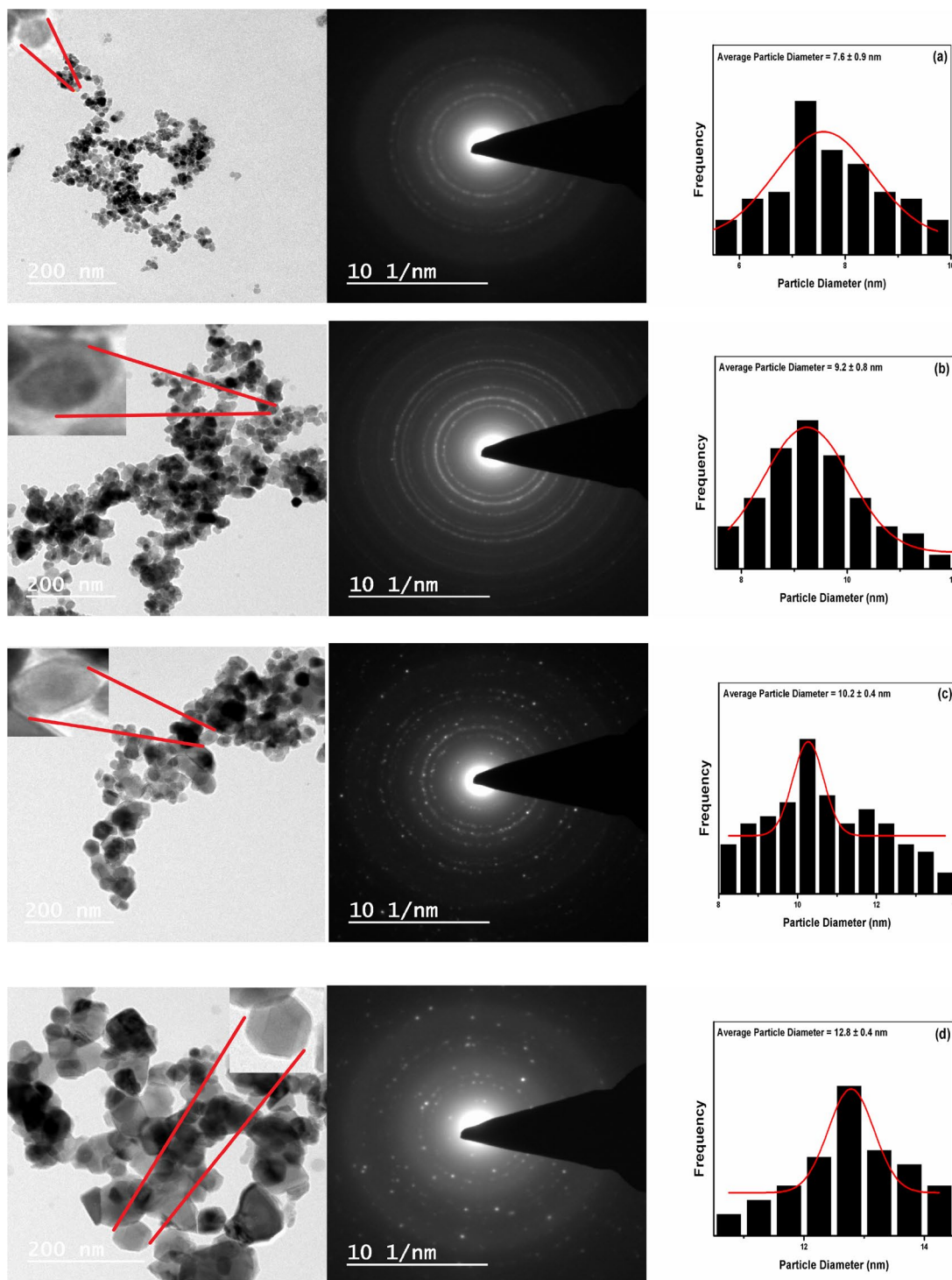


**Fig. 6** Transmission electron microscope images and corresponding particle size histograms of cobalt ferrite samples annealed at **a** 400 °C, **b** 600 °C, **c** 700 °C, **d** 800 °C

inference drawn from the IR spectra, that the samples are free from  $\text{OH}^-$  ions at higher temperatures. Thus, the overall thermal analysis of the sample has clearly elucidated the detailed changes (including structural modifications) taking

place in the sample with the temperature. This information would be predicted to be useful in analyzing the variation of the magnetic properties of the sample with temperature reported in the later part of this manuscript. We, further,

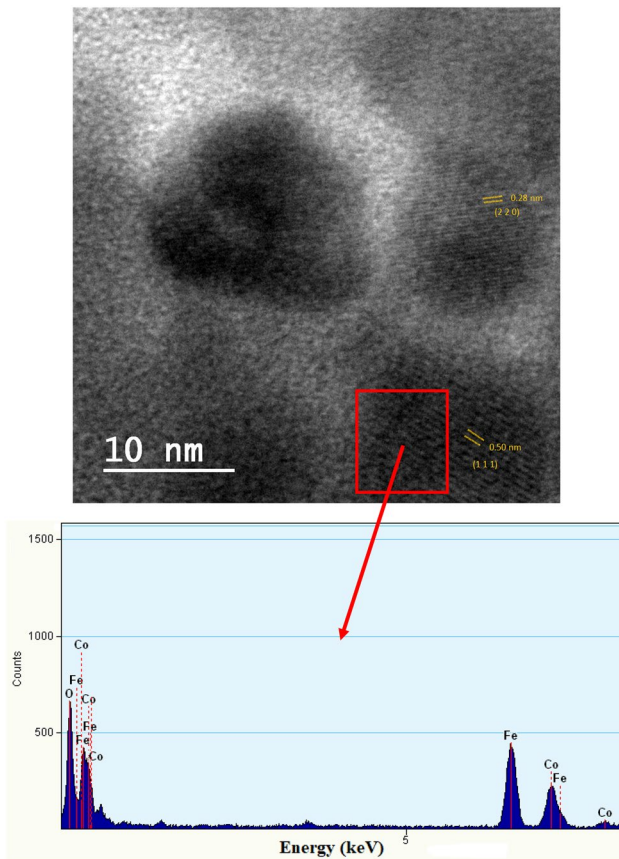


**Fig. 7** High resolution transmission electron microscope image and EDS analysis of cobalt ferrite sample annealed at 400 °C

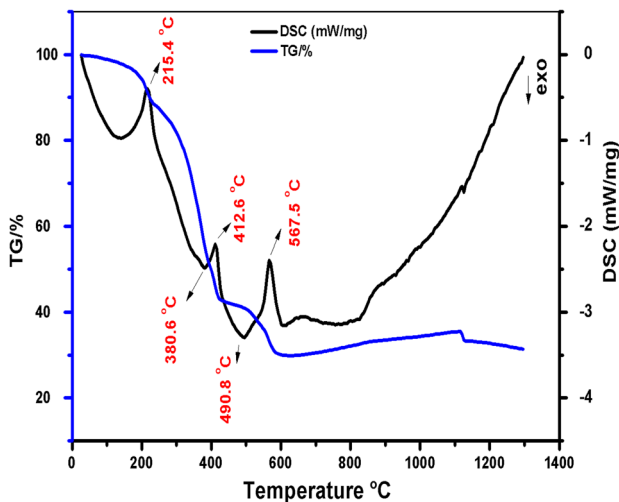


**Fig. 8** TG-DSC plot of the as prepared dark brown gel

have observed a slight increment of mass of the sample in thermogram between 800 °C and 1000 °C; this increment is insignificant and may be due to the Archimedes' effect. If

there is a small variation in the rate of heating during recording of the thermograms there is a possibility for getting such small increment in the mass.

### 3.5 Magnetic properties

With a view to assess the magnetic behavior of the cobalt ferrite nanoparticles, we have recorded hysteresis loops of all the samples at ambient temperature using vibrating sample magnetometer and presented in Fig. 9. From the hysteresis loops, various magnetic parameters viz., saturation magnetization ( $M_s$ ), coercive field ( $H_c$ ) and reduced remnant magnetization ( $R = M_r/M_s$ ) are evaluated and presented in Table 2. The non-zero value of remnant magnetization,  $M_r$  and considerably high value of  $H_c$ , are the general characteristics hard ferro- or ferri-magnetic materials. The obtained values of remnant magnetization ( $M_r$ ) and coercive field ( $H_c$ ) for the studied nanosized (Table 2) samples suggest that the developed cobalt ferrite nanoparticles fall under the above-mentioned categories. Moreover, we have also observed increase of  $H_c$  with increase of particle size. The maximum value of  $H_c$  is found to be 2214 Oe for the particles of average size ~ 10 nm. For the cobalt ferrite nanoparticles of still higher dimensions, the value of  $H_c$  is found to be lower. To be mentioned in detail, for the nanoparticles of the average size 12.8 nm, the value of  $M_s$  is reached to an extraordinary higher value (85.5 emu/g) and the corresponding coercive field is found to be 1920 Oe (Fig. 10). The inference of this behavior is that there is a transition of the state of the material from single-domain to multi-domain (a transition associated with the orientation of domain wall) [21, 26, 40, 41]. The high-resolution transmission electron microscope image

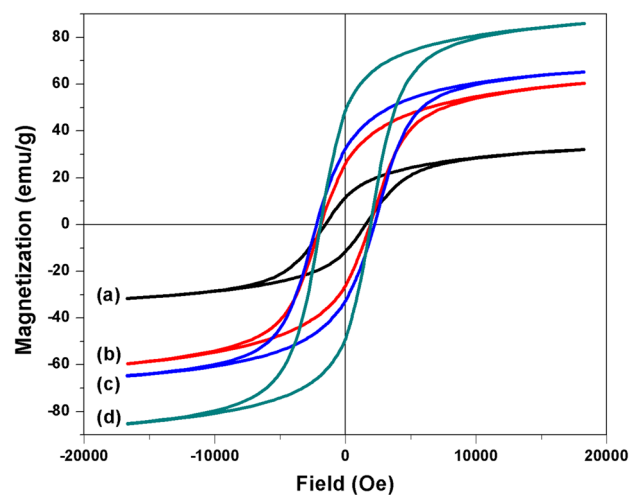


**Fig. 9** Room temperature hysteresis curves of cobalt ferrite samples annealed at **a** 400 °C, **b** 600 °C, **c** 700 °C, **d** 800 °C

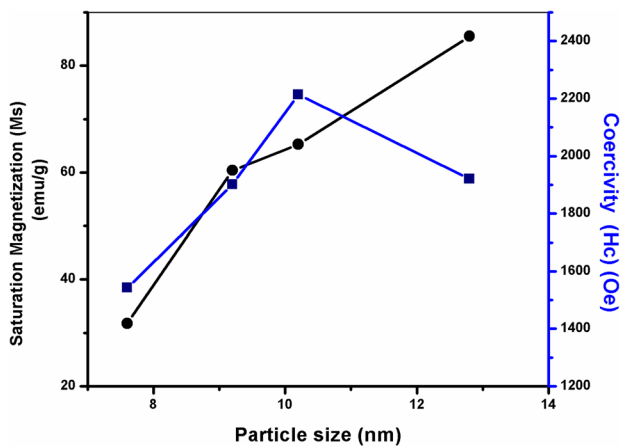


**Fig. 10** Variation of saturation magnetization and coercivity of cobalt ferrite samples with particle size

of the sample annealed at 400 °C (Fig. 7), clearly indicates the presence of cobalt ferrite nanoparticles in single-domain state.

To throw more light on the magnetic characteristics of the studied samples, we have evaluated the magneto-crystalline anisotropy constant,  $K$ , using Stoner–Wohlfarth relation,

$$H_c = 2K/M_s, \quad (2)$$

for the cobalt ferrite nanoparticles annealed at different temperatures. The value of  $K$  is observed to increase with particle size. The maximum value of  $K$  for the sample with average particle size of 12.8 nm is estimated to be  $10.74 \times 10^6 \text{ erg/cm}^3$  (Table 2); this value of  $K$  is nearly equal to that of bulk single phase  $\text{CoFe}_2\text{O}_4$  reported by other authors [42]. Further it may be noted here, with the decrease of particle size (from 12.8 nm) the value of  $K$  is found to decrease rather than remaining invariant as reported earlier [43]. This discrepancy of change of the intrinsic magnetic anisotropy arises due to variations in the (i) particle size, (ii) shape and (iii) also due to inter particle interactions [15].

To know the performance of the studied  $\text{CoFe}_2\text{O}_4$  nanoparticles as permanent magnets, we have drawn  $B$  (or  $4\pi M$ ) vs  $H$  plots. Figure 11 represents such plot for the cobalt ferrite nanoparticles of size 12.8 nm obtained at annealing temperature of 800 °C. From these plots, we have evaluated the maximum magnetization energy  $(BH)_{\text{max}}$  (or figure of merit of permanent magnets) and its variation with the average size of the particles is plotted in Fig. 12. The magnitude of  $(BH)_{\text{max}}$  is found to be the maximal (1.04 MGOe or  $8.28 \text{ kJm}^{-3}$ ) for the  $\text{CoFe}_2\text{O}_4$  nanoparticles of average particle size 12.8 nm. The obtained maximal value of  $(BH)_{\text{max}}$  is found to be well with the range of earlier reported values (0.5 up to 1.1 MGOe) for cobalt ferrite particles synthesized by different other methods [44].

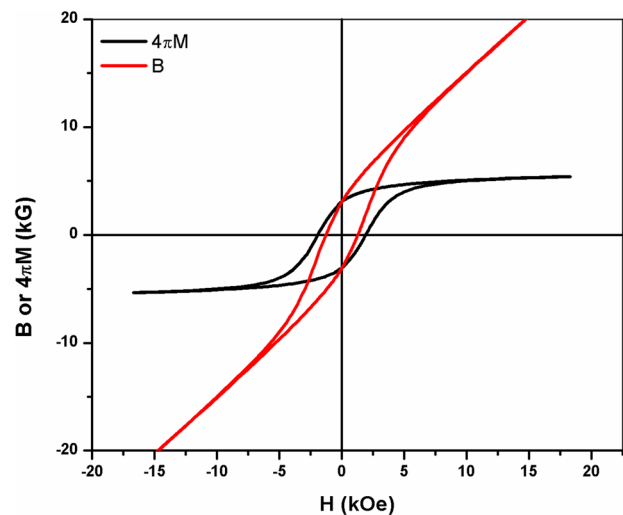


**Fig. 11**  $B$  (or)  $4\pi M$  vs.  $H_c$  loops of cobalt ferrite nanoparticles annealed at 800 °C

In Fig. 12, the variation of anisotropy constant  $K$  vs average particle size is also plotted. The dependence of  $K$  with the particle size is found to be similar to that of the parameter  $(BH)_{\text{max}}$ . This observation suggests that there is a strong relationship between these two parameters. This result may be attributed to the large magnetic moment of the studied samples. Further, we have already mentioned that if the size of the cobalt ferrite nanoparticles is lower than 10 nm (obtained for the samples annealed below 700 °C), they are confined to the single-domain state; for these samples the coercivity,  $H_c$ , (the parameter on which the values of  $K$  as well as  $(BH)_{\text{max}}$  are dependent) is found to be larger than  $2\pi M_s$ . To be in detail, for the sample annealed at 700 °C, the value of  $H_c$ , is estimated to be 2214 G while that of  $2\pi M_s$  is

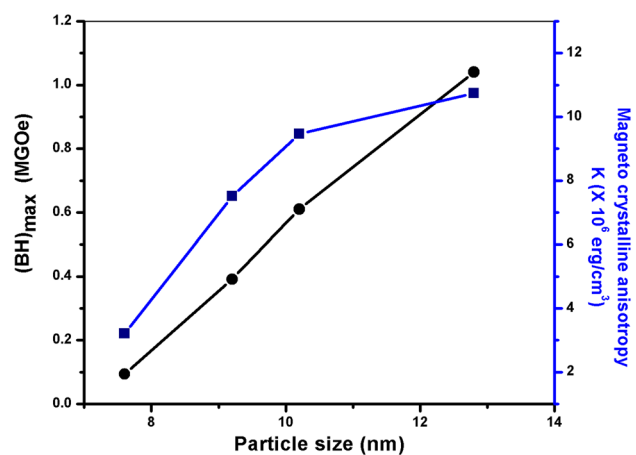


**Fig. 12** Variation of  $(BH)_{\text{max}}$  and Magneto-crystalline anisotropy of cobalt ferrite nanoparticles with particle size



found to be 2051 G. This inference suggests that the value of  $(BH)_{\max}$  is dependent on  $M_s$  [27].

For further increase of annealing temperature ( $> 700$  °C), the values  $(BH)_{\max}$  and  $M_s$  are found to be still higher; however for such samples, the value of  $H_c$  is found to be less than  $2\pi M_s$ ; this is probably due to confinement of the state of the particles to multi-domain. Over all, the prepared cobalt ferrite nanoparticles by this method have exhibited high coercivity, higher magnetization and large cubic magneto-crystalline anisotropy. Hence the studied cobalt nanoferrite (prepared by sol–gel method with PEG as chelating agent) is highly useful for the applications in magnetic recording, high density digital recording disks and in magnetic sensor and are advantageous over the conventional RE mixed ferrites [45–49]. However, for using these materials for biomedical applications (e.g., hyperthermia, drug delivery etc.) the material should exhibit super-paramagnetic behavior (which means no energy loss during demagnetization or  $H_c$  should be zero), in the present investigation, such behavior could not be visualized. Probably the size of the particles should be further reduced (to  $\sim 2$ – $4$  nm [33, 40]) for achieving this. This we could not get using PEG as chelating agent. Attempts with other chelating agents with different experimental conditions are necessary to make the material to exhibit such super-paramagnetic character. We are extending the investigations along these lines and planned to communicate in due course.

## 4 Conclusions

This study confirms that polyethylene glycol (PEG) assisted sol–gel (with subsequent annealing) method is one of the best methods to achieve single-domain  $\text{CoFe}_2\text{O}_4$  nanoparticles with larger saturation magnetization at an optimal annealing temperature. The developed cobalt ferrite nanoparticles are observed to be highly dispersed with uniform shape. The magnetic properties of these nanoparticles studied as functions of the average particle size and annealing temperature indicated that the saturation magnetization  $M_s$  and remnant magnetization  $M_r$  increase monotonously with the increase in the size of the nanoparticles and found to reach the higher values, 85.5 emu/g and 49 emu/g, respectively, for the particles of the size 12.8 nm. The variation of coercive field with the particle size exhibited a non-monotonic behavior with distinct maximum (2214 Oe) with moderate magnetization, 62.7 emu/g for the cobalt ferrite containing the nanoparticle of average size  $\sim 10$  nm and indicated that the particles are confined to single-domain. Moreover, the studied cobalt ferrite nanoparticles have exhibited the highest magneto-crystalline anisotropy constant,  $K$ , ( $10.74 \times 10^6$  erg/cm<sup>3</sup>) and the maximum value of  $(BH)_{\max}$  (1.04 MGOe) for the particles with size  $\sim 12.8$  nm.

These values suggest the superior potentiality of the studied rare-earth (RE) free cobalt ferrite nanoparticles for the applications in magnetic recording, high density digital recording disks and in magnetic sensors.

**Acknowledgements** The authors acknowledge help rendered by IIC-IIT Roorkee in recording TEM images. The authors also wish to thank SAIF-IIT Madras and SAIF-IIT Bombay for extending the facility to record TG-DSC and FTIR.

## References

1. B.H. Sohn, R.E. Cohen, Processible optically transparent block copolymer films containing superparamagnetic iron oxide nanoclusters. *Chem. Mater.* **9**, 264–269 (1997)
2. M. Safarik, Safarikova, Magnetic nanoparticles and biosciences, in *Nanostructured materials*, ed. by H. Hofmann, Z. Rahman, U. Schubert (Springer, Vienna, 2002), pp. 1–23
3. K.M. Krishnan, A.B. Pakhomov, Y. Bao, P. Blomqvist, Y. Chun, M. Gonzales, K. Griffin, X. Ji, B.K. Roberts, Nanomagnetism and spin electronics: materials, microstructure and novel properties. *J. Mater. Sci.* **41**, 793–815 (2006)
4. N.M. Deraz, Size and crystallinity-dependent magnetic properties of copper ferrite nano-particles. *J. Alloys Compd.* **501**, 317–325 (2010)
5. M. Pita, J.M. Abad, C. Vaz-Dominguez, C. Briones, E. Mateo-Marti, J.A. Martin-Gago, M. del Puerto Morales, V.M. Fernandez, Synthesis of cobalt ferrite core/metallic shell nanoparticles for the development of a specific PNA/DNA biosensor. *J. Colloid Interface Sci.* **321**, 484–492 (2008)
6. G. Balaji, R. Aravinda Narayanan, A. Weber, F. Mohammad, C.S.S.R. Kumar, Giant magnetostriction in magnetite nanoparticles. *Mater. Sci. Eng. B* **177**, 14–18 (2012)
7. J. Liu, H. Liang, Yi Zhang, Wu Guanglei, Wu Hongjing, Facile synthesis of ellipsoid-like  $\text{MgCo}_2\text{O}_4/\text{Co}_3\text{O}_4$  composites for strong wideband microwave absorption application. *Compos B* **176**, 107240 (2019)
8. Wu Hongjing, M. Qin, L. Zhang,  $\text{NiCo}_2\text{O}_4$  constructed by different dimensions of building blocks with superior electromagnetic wave absorption performance. *Compos. B* (2019). <https://doi.org/10.1016/j.compositesb.2019.107620>
9. D. Ghanbari, M. Salavati-Niasari, M. Ghasemi-Kooch, A sonochemical method for synthesis of  $\text{Fe}_3\text{O}_4$  nanoparticles and thermal stable PVA-based magnetic nanocomposite. *J. Ind. Eng. Chem.* **20**, 3970–3974 (2014)
10. N.M. Deraz, A. Alarifi, Novel preparation and properties of magnesianoferrite nanoparticles. *J. Anal. Appl. Pyrolysis* **97**, 55–61 (2012)
11. D. Chen, Hong yan Liu, Lin Li, One-step synthesis of manganese ferrite nanoparticles by ultrasonic wave-assisted ball milling technology. *Mater. Chem. Phys.* **134**, 921–924 (2012)
12. W.F. Brown, Thermal fluctuations of a single-domain particle. *Phys. Rev.* **130**, 1677–1686 (1963)
13. A.C. Lima, M.A. Morales, J.H. Araújo, J.M. Soares, D.M.A. Melo, A.S. Carrico, Evaluation of  $(BH)_{\max}$  and magnetic anisotropy of cobalt ferrite nanoparticles synthesized in gelatin. *Ceram. Int.* **41**, 11804–11809 (2015)
14. A.H. Morrish, *The physical principles of magnetism* (Wiley-VCH, Germany, 2001)
15. M. Shi, R. Zuo, Y. Xu, Y. Jiang, G. Yu, H. Su, J. Zhong, Preparation and characterization of  $\text{CoFe}_2\text{O}_4$  powders and films via the sol–gel method. *J. Alloys Compd.* **512**, 165–170 (2012)

16. K. Maaz, A. Mumtaz, S.K. Hasanain, A. Ceylan, Synthesis and magnetic properties of cobalt ferrite (CoFe<sub>2</sub>O<sub>4</sub>) nanoparticles prepared by wet chemical route. *J. Magn. Magn. Mater.* **308**, 289–295 (2007)
17. L. Victoria, C.C. Ddel, C. Rinaldi, Synthesis and magnetic characterization of cobalt-substituted ferrite (Co<sub>x</sub>Fe<sub>3-x</sub>O<sub>4</sub>) nanoparticles. *J. Magn. Magn. Mater.* **314**, 60–67 (2007)
18. F. Khatkhatay, Enhanced flux pinning properties in self-assembled magnetic CoFe<sub>2</sub>O<sub>4</sub> nanoparticles doped YBa<sub>2</sub>Cu<sub>3</sub>O<sub>7</sub> thin films. *IEEE Trans. Appl. Supercond.* **23**, 8001204 (2013)
19. D. Chen, X. Yi, Z. Chen, Y. Zhang, B. Chen, Z. Kang, Synthesis of CoFe<sub>2</sub>O<sub>4</sub> nanoparticles by a low temperature microwave-assisted ball-milling technique. *Int. J. Appl. Ceram. Tech.* **11**, 954–959 (2013)
20. M.H. Khedr, A.A. Omar, S.A.A. Moaty, Magnetic nanocomposites: preparation and characterization of co-ferrite nanoparticles. *Colloids Surf. A Physicochem. Eng. Asp.* **281**, 8–14 (2006)
21. Q. Song, Z.J. Zhang, Shape control and associated magnetic properties of spinel cobalt ferrite nanocrystals. *J. Am. Chem. Soc.* **126**, 6164–6168 (2004)
22. C.N. Chinnasamy, B. Jayadevan, K. Shinoda, K. Tohji, D.J. Djayaprawira, M. Takahashi, R.J. Joseyphus, A. Narayanasamy, unusually high coercivity and critical single-domain size of nearly monodispersed CoFe<sub>2</sub>O<sub>4</sub> nanoparticles. *Appl. Phys. Lett.* **83**, 2862 (2003)
23. M. Sangmanee, S. Maensiri, Nanostructures and magnetic properties of cobalt ferrite (CoFe<sub>2</sub>O<sub>4</sub>) fabricated by electrospinning. *Appl. Phys. A* **97**, 167–177 (2009)
24. S. Zinatloo-Ajabshir, M. Salavati-Niasari, Preparation of magnetically retrievable CoFe<sub>2</sub>O<sub>4</sub>@SiO<sub>2</sub>@Dy<sub>2</sub>Ce<sub>2</sub>O<sub>7</sub> nanocomposites as novel photocatalyst for highly efficient degradation of organic contaminants. *Compos. Part B Eng.* **174**, 106930 (2019)
25. A.F. Junior, E.C.O. Lima, A.M. Novak, P.R. Wells Jr., Synthesis of nanoparticles of Co<sub>x</sub>Fe<sub>3-x</sub>O<sub>4</sub> by combustion reaction method. *J. Magn. Magn. Mater.* **308**, 198–202 (2007)
26. G.R. Patta, V. Ravi Kumar, K.H. Rao, N. Veeraiah, Synthesis and studies on magnetic properties of single-phase cobalt ferrite nanoparticles—influence of content of chelating agent. *Appl. Phys. A* **125**, 187 (2019)
27. A.M. Cojocariu, M. Soroceanu, L. Hrib, V. Nica, O.F. Caltun, Microstructure and magnetic properties of substituted (Cr, Mn)—cobalt ferrite nanoparticles. *Mater. Chem. Phys.* **135**, 728–732 (2012)
28. M. Eshraghi, P. Kameli, Magnetic properties of CoFe<sub>2</sub>O<sub>4</sub> nanoparticles prepared by thermal treatment of ball-milled precursors. *Curr. Appl Phys.* **11**, 476–481 (2011)
29. M. Salavati-Niasari, F. Davar, M.R. Loghman-Estarki, Controllable synthesis of thioglycolic acid capped ZnS(Pn)0.5 nanotubes via simple aqueous solution route at low temperatures and conversion to wurtzite ZnS nanorods via thermal decompose of precursor. *J. Alloys Compd.* **494**, 199–204 (2010)
30. E.L.S. Solomon, A.R. Natarajan, A.M. Roy, V. Sundararaghavan, A. Van der Ven, E.A. Marquis, Stability and strain-driven evolution of β' precipitate in Mg-Y alloys. *Acta Mater.* **166**, 148–157 (2019)
31. K.S. Rao, G.S.V.R.K. Choudary, K.H. Rao, Ch. Sujatha, structural and magnetic properties of ultrafine CoFe<sub>2</sub>O<sub>4</sub> nanoparticles. *Procedia Mater. Sci.* **10**, 19–27 (2015)
32. K. Venkateswarlu, A. Chandra Bose, N. Rameshbabu, X-ray peak broadening studies of nanocrystalline hydroxyapatite by Williamson–Hall analysis. *Phys B* **405**, 4256–4261 (2010)
33. I. Sharifi, H. Shokrollahi, M.M. Doroodmand, R. Safi, Magnetic and structural studies on CoFe<sub>2</sub>O<sub>4</sub> nanoparticles synthesized by co-precipitation, normal micelles and reverse micelles methods. *J. Magn. Magn. Mater.* **324**, 1854–1861 (2012)
34. M.G. Naseri, E.B. Saion, H.A. Ahangar, A.H. Shaari, M. Hashim, Simple synthesis and characterization of cobalt ferrite nanoparticles by a thermal treatment method. *J. Nanomater.* **2010**, 1167–1174 (2010)
35. P. Sobhanachalam, Ch. Vijaya Kumari, G. Sahaya Baskaran, P. Syam Prasad, N. Veeraiah, V. Ravi Kumar, On identifying efficient modifier oxide in improving bioactivity of Fe<sub>2</sub>O<sub>3</sub> doped calcium oxy fluoroborophosphate glasses. *J. Alloys Compd.* **692**, 219–226 (2017)
36. L.B. Newalkar, S. Komarneni, H. Katsuki, Microwave-hydrothermal synthesis and characterization of barium titanate powders. *Mater. Res. Bull.* **36**, 2347–2355 (2001)
37. Y.J. Kwon, K.H. Kim, C.S. Lim, K.B. Shim, Characterization of ZnO nanopowders synthesized by the polymerized complex method via an organochemical route. *J. Ceram. Process. Res.* **3**, 146–149 (2002)
38. N.M. Deraz, Production and characterization of pure and doped copper ferrite nanoparticles. *J. Anal. Appl. Pyrolysis* **82**, 212–222 (2008)
39. L. Li, H. Liu, Y. Wang, J. Jiang, F. Xu, Preparation and magnetic properties of Zn–Cu–Cr–La ferrite and its nanocomposites with polyaniline. *J. Colloid Interface Sci.* **321**, 265–271 (2008)
40. K. Srinivasa Rao, S.V. Ranga Nayakulu, M. Chaitanya Varma, G.S.V.R.K. Choudary, K.H. Rao, Controlled phase evolution and the occurrence of single domain CoFe<sub>2</sub>O<sub>4</sub> nanoparticles synthesized by PVA assisted sol-gel method. *J. Magn. Magn. Mater.* **451**, 602–608 (2018)
41. G. Jian, Q. Fu, D.J. Zhou, Particles size effects of single domain CoFe<sub>2</sub>O<sub>4</sub> on suspensions stability. *J. Magn. Magn. Mater.* **324**, 671–676 (2012)
42. H. Shenker, Magnetic anisotropy of cobalt ferrite (Co<sub>1.01</sub>Fe<sub>2.00</sub>O<sub>3.62</sub>) and nickel cobalt ferrite (Ni<sub>0.72</sub>Fe<sub>0.20</sub>Co<sub>0.08</sub>Fe<sub>2</sub>O<sub>4</sub>). *Phys. Rev.* **107**, 1246–1249 (1957)
43. E.C. Stoner, E.P. Wohlfarth, A mechanism of magnetic hysteresis in heterogeneous alloys. *Philos. Trans. R. Soc. A Math. Phys. Eng. Sci.* **240**, 599–642 (1948)
44. F.D.A.O. Cabral, F.L.A. Machado, J.H. Araujo, J.M. Soares, A.R. Rodrigues, A. Araujo, Preparation and magnetic study of the CoFe<sub>2</sub>O<sub>4</sub>–CoFe<sub>2</sub> nanocomposite powders. *IEEE Trans. Magn.* **44**, 4235–4238 (2008)
45. X. Zhou, Y. Zhou, L. Zhou, J. Wei, J. Wu, D. Yao, Effect of Gd and La doping on the structure, optical and magnetic properties of NiZnCo ferrites. *Ceram. Int.* **45**, 6236–6242 (2019)
46. M.M.N. Ansari, S. Khan, N. Ahmad, Effect of R<sup>3+</sup> (R = Pr, Nd, Eu and Gd) substitution on the structural, electrical, magnetic and optical properties of Mn–ferrite nanoparticles. *J. Magn. Magn. Mater.* **465**, 81–87 (2018)
47. P. Venkata Sreenivas, A. Shiva, C.V. Ramana, Chemical bonding and magnetic properties of gadolinium (Gd) substituted cobalt ferrite. *J. Alloys Compd* **644**, 470–475 (2015)
48. G. Ganapathi Rao, B. Lakshmi Rekha, K.N. Chidambara Kumar, V. Nirupama, D. Madhavaprasad, Effect of Gd and Nb on dielectric and magnetic transition temperature of BaTiO<sub>3</sub>–Li<sub>0.5</sub>Fe<sub>2.5</sub>O<sub>4</sub> composites. *Phys. B* **560**, 1–5 (2019)
49. A.L. Ortega, E. Lottini, C.J. Fernandez, Sangregorio, exploring the magnetic properties of cobalt-ferrite nanoparticles for the development of a rare-earth-free permanent magnet. *Chem. Mater.* **27**, 4048–4056 (2015)
50. J.G. Lee, J.Y. Park, C.S. Kim, Growth of ultra-fine cobalt ferrite particles by a sol-gel method and their magnetic properties. *J. Mater. Sci.* **33**, 3965–3968 (1998)
51. M.E. Mata-Zamora, H. Montiel, G. Alvarez, J.F. Barrona, H. Arriola, J.M. Saniger, R. Valenzuela, Remanence of the interparticle interactions and its influence on the microwave absorption in Co-ferrite. *J. Magn. Magn. Mater.* **320**, e139–e142 (2008)

52. E. Veena Gopalan, P.A. Joy, I.A. Al-Omari, D. Sakthi Kumar, M.Y. Yoshida, R. Anantharaman, On the structural, magnetic and electrical properties of sol-gel derived nanosized cobalt ferrite. *J. Alloys Compd* **485**, 711–717 (2009)
53. M. Gharagozlou, Synthesis, characterization and influence of calcination temperature on magnetic properties of nanocrystalline spinel Co-ferrite prepared by polymeric precursor method. *J. Alloys Compd.* **486**, 660–665 (2009)
54. P.S. Aghav, V.N. Dhage, M.L. Mane, D.R. Shengule, R.G. Dorik, K.M. Jadhav, Effect of aluminum substitution on the structural and magnetic properties of cobalt ferrite synthesized by sol-gel auto combustion process. *Phys. B* **406**, 4350–4354 (2011)
55. S.R. Naik, A.V. Salker, S.M. Yusuf, S.S. Meena, Influence of Co<sup>2+</sup> distribution and spin-orbit coupling on the resultant magnetic properties of spinel cobalt ferrite nanocrystals. *J. Alloys Compd.* **566**, 54–61 (2013)

**Publisher's Note** Springer Nature remains neutral with regard to jurisdictional claims in published maps and institutional affiliations.